Mammogram breast cancer segmentation and classification using Hierarchical Fuzzy C Means – Modified Expectation Maximization algorithm and deep convolutional neural network

A.Anbumani[1] • Dr.P.Suresh Kumar[2]
[1]anbuinfo2006@gmail.com, [2]sureshkumarp@mahendra.info
[1] Department of CSE, Erode Sengunthar Engineering College, Erode, Tamilnadu, India
[2] Department of EEE, Mahendra Engineering College (Autonomous), Namakkal, Tamilnadu, India

Keywords: 2DGGIF, NSCT, GLRM, DCNN, Classification, Segmentation.

DOI Number:10.14704/nq.2022.20.8.NQ44508 **NeuroQuantology 2022; 20(8): 4821-4838**

1 INTRODUCTION

Among different types of cancer the most common type that affects mostly the women is Breast cancer. It is estimated to contribute around 14% of the total deaths [1]. World Health Organization has reported that around 13.7% of the women die due to breast cancer [2]. Hence, early detection of this type of cancer is highly essential so that treatment can be started at an early stage [3][4][5][6]. The recent improvements in the field of photography have introduced the mammogram images. These images have the capacity to capture the masses in the breast regions with good resolution [7][8]. Many techniques have been presented so far for categorizing these mammogram images into two categories that is, benign or malignant [9][4][10]. Breast cancer is a disease that has chances of around 90% for complete treatment and recovery if the treatment is started at the early stage. Based on the state in which it is identified, the survival rate will vary. The survival rate is very high for the patients who are identified at the very initial stage [11]. Deep learning techniques are popularly used for breast cancer detection in the recent days [12][13]. Hence, development of a framework that is capable of accurately classifying the mammogram data is a vital task.

Hence, in this research a novel framework for detection of breast cancer using mammogram data isproposed.

The contributions done in this work are as follows:

a) A new classification framework for the classification of breast images is presented.
b) A new restoration algorithm called 2D Auto encoder-based Guided Image Filter (2D AGIF) algorithm is proposed.
c) A novel image enhancement technique using Bayes Shrink-based Non-Sub-sampled Contourlet Transform (BS-NSCT) is proposed.
d) A new image segmentation technique using Hierarchical Fuzzy C Means Gaussian Snake Model (HFC-GSM) algorithm is presented.
e) The proposed framework was evaluated quantitatively using metrics like MSE, PSNR, Jaccard coefficient, Dice coefficient, SSIM, accuracy, specificity, precision, recall and

precision.

The remaining section of the work is organized in the following way. Section 2 elaborates the literature survey of the previous works related to proposed idea. Section 3 shows the proposed methodology. The results and discussion are performed in Section 4. At the end conclusion section is provided.

2 RELATED WORK

A system for classification of mammogram images into 4 categories was proposed by the authors in [14]. In this work, the combinations of various enhancement and segmentation techniques were analyzed and evaluated. This system achieved a classification accuracy of about 90.7%. The overall sensitivity achieved by this framework was about 96.2%. An integrated system for breast image classification using deep learning was proposed in [15]. Here, a new deep learning model was proposed for the segmentation of breast images. 4 -fold cross validation technique was opted in this paper. All the analysis was performed using INbreast dataset. This system achieved an overall classification accuracy of 95.64%.

Analysis of dual energy mammogram images was performed in [16]. In this work, the mammogram images were obtained from women before biopsy and used for analysis. Three different analysis was performed. The first analysis was performed using water-protein images. The second analysis was performed using mammogram images and the third analysis was performed using a combination of the two types of images. Here, 10 -fold cross validation technique was employed. Detection of breast cancer based on deep learning was given in [17]. In this work evaluation was performed on the publicly available CBIS-DDSM dataset. Here, single model system achieved an area under the curve value of 0.88 and the four model attained AUC of about 0.91. It was observed that, the annotations were requiredonly during the initial stages.

A technique for detection of breast cancer based on Hough transform was proposed in [18]. Classification was performed based on support vector machine classifier. Around 94% classification accuracy was achieved here. Comparison was performed using Linear Discriminant Analysis classifier that could achieve only 86% accuracy. Another framework for breast image classification was presented in [19]. Here images were classified into three categories namely the benign, malignant and the normal. This system attained a classification accuracy of about 90.50%. Also, the area under the curve value reached was
0.9. The tumor patches were manually labelled and trained in this system.

A technique for the prediction of breast cancer using deep learning was explored in [20]. Among 71 mammogram images, around 34 images were identified to be false negative images in this framework. This work achieved a recall value of 87%. The usage of artificial intelligence (AI) in breast cancer classification was analyzed in [21]. Here, a brief reviewwas presented on various current techniques available and the future prospects of artificial intelligence and deep learning techniques on the breast cancer detection. In addition to classification, analysis of AI was performed for risk prediction, selection of treatment, denoising, etc.

Multiview CNN was used for cancer prediction in [22]. Here, instead of using a single image, multiple images were captured from various orientations. These images were merged to perform prediction. In addition to conventional convolution, dilated convolution was employed in this paper. The classification accuracy of this framework was enhanced using a penalty function. Detection of breast cancer using DWT and GLCM matrix was proposed in [23]. Here, initially the images were segmented to obtain the region of interest. From the segmented region DWT was applied. Using the DWT coefficients, the GLCM matrix features were extracted and then classified.

Usage of data augmentation technique for the classification of mammogram images was presented in [24]. In this work, the

generative adversarial networks (GANs) were employed for augmentation of the mammogram images. Classification was performed using ResNet classifier. AUC of about 0.896 was achieved by this system. Mammogram classification using BPNN was proposed in [25]. Here, initially the mammogram images were enhanced using sigmoid function. Then, the feature extraction was performed using GLCM matrix features. From these features, classification was performed using BPNN classifier. This system attained 96.3% accuracy.

A review was done by authors [26] on various deep learning techniques for breast cancer detection. Here, a new model for feature mapping was also proposed. The various challenges in this field were also discussed in this paper. Also, the techniques used for cancer detection using histopathology images were also discussed in this work. A technique for the classification of histology images was presented in [27]. Initially patch prediction was done. Then the ensemble fusion was performed. Classification was performed using logistic regression. This system achieved around 12.5% higher accuracy than the state-of-the-art works in the literature.

3. PROPOSED METHODOLOGY

The proposed methodology shown in fig.1 comprises of steps like image preprocessing (restoration and enhancement), segmentation, feature extraction and classification. This is depicted in Figure 1. The noisy mammogram image is initially acquired. This image is pre- processed using restoration and enhancement. Image restoration is done to remove noise and enhancement is done to increase the contrast and details of the image. By using image segmentation the Region Of Interest (ROI) is segmented for further processing. Then, from the segmented regions, the image is classified to two groups namely benign and malignant.

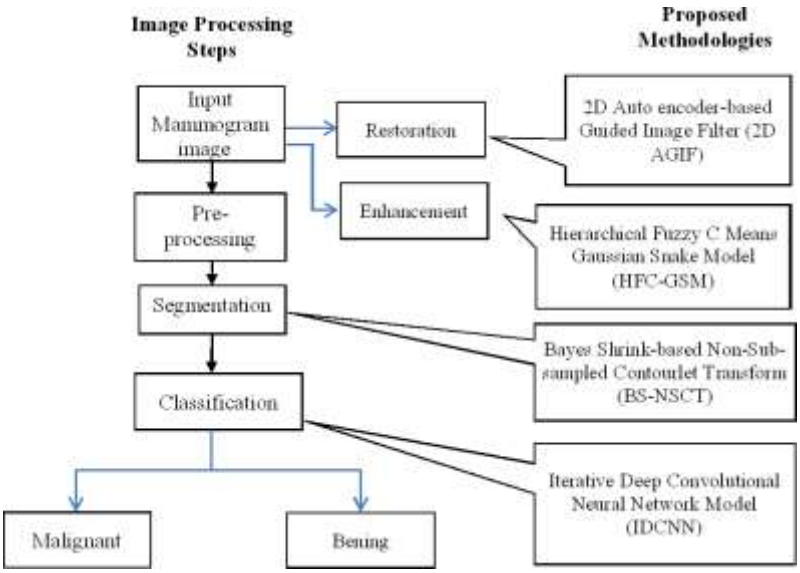

Figure 1. Flow chart of the proposed breast image classification methodology

Image Pre-processing

Pre-processing was performed using two steps namely, restoration and enhancement. Image restoration was performed using the proposed 2D Auto encoder-based Guided Image Filter (2D AGIF) and enhancement was performed using Bayes Shrink-based Non-Sub-sampled Contourlet Transform (BS-NSCT).

Image Restoration using 2D Auto encoder-based Guided Image Filter (2D AGIF).

The input image is filtered using 2D Auto encoder-based Guided Image Filter (2D AGIF). The conventional Guided Image filtering process increases the capability to recover the edge and detail information of an image. Therefore, it is

popularly used for noise removal applications. It is performed as follows.

Let us consider s to be the input image that must be denoised. Let I_i represent the input guided image. Then the denoised image can be obtained using,

$r_i = a_j I_i + b_j, \forall j$ (1)

$r_i = s_i + n_i$ (2)

Here, r represents the denoised image, ω_j represents the square window patch with the center pixel j and a,b are the linear coefficients. To determine the values of the coefficients a,b, the following function must be optimized.

$$a,b = \min_{a,b}[(a I + b - s)^2 + \varepsilon a^2] \quad (3)$$

The above equation is solved using Least Square technique to obtained the coefficients as follows

$$a = \frac{1}{|\omega|} \sum_{i \in \omega_j} I_i s_i - m_j s_j / [sd^2 + \varepsilon] \quad (4)$$

j $|\omega|$ $\bar{\omega}$ i i j j ω j
ω $i \in \omega_j$ ω

$$b_j = s_j - a_j m_j - \quad (5)$$

In the above equations, m_j represents the mean and sd^2 represents the standard deviation of the pixels in the window region ω_j.

Finally, the denoised image is computed as,

$$r_i = \frac{1}{|\omega|} \sum_{j / i \in \omega_k} [a_j I_i + b_j] \quad (6)$$

To further improve the quality of denoising, in the proposed 2D AGIF scheme, odified Equation 3, using weight $w_{i^{th}}$. The term $w_{i,j}$ is the weight between the and the center j^{th} pixel.

i,j i,j

$$a,b = \min_{a,b} w_{i,j} [(a I + b - s)^2 + \varepsilon a^2] \quad (7)$$

The weighing function $w_{i,j}$ is defined based on denoising auto encoders. Denoising auto encoders are incorporated in this work as they produce the output based on the mean of the true data density. Thus, they are effective in the removal of noise based on the auto encoder error. The weighting function is computed by the minimization of the following equation

$$w_{i,j} = \min M [\| I_i (I_i - o_i) \|^2] \quad (8)$$

Where I_i represents the input image, I_O represents the filtered output image, M_i represents the mean image value and $\square$ is the Gaussian noise.

Image Enhancement using Bayes Shrink-based NSCT Transform (BS-NSCT)

The filtered images were then enhanced using Bayes Shrink-based Non-Sub-sampled Contourlet Transform (BS-NSCT). Image enhancement is essential as it highlights the ROI of the image. Transforms like Wavelet transform, Curvelet transform have been used in the literature for image enhancement. Though Wavelet transform enhances the discontinuities present in the image, it does not enhance the contour regions of the image. This drawback can be eliminated by the usage of Curvelet transform. However, Curvelet transform can be best implemented in frequency and not in the discrete domain. Hence, to overcome all these drawbacks, in this work, we have used the Non-Sub- sampled Contourlet Transform[28]. This technique is based on pyramids and filter banks. It comprises of analysis and synthesis filters. In this technique, the following condition must be satisfied.

$$H_O(Z)G_O(Z) \square H_1(Z)G_1(Z) \square 1 \quad (9)$$

Let us consider that the restored image be represented as $I^R \square R^{M \square N}$. Then, the output of the enhancement operation is represented as $I^E \square R^{M \square N}$. The two-channel decomposition of the NSCT pyramid structure is shown in Figure 2.

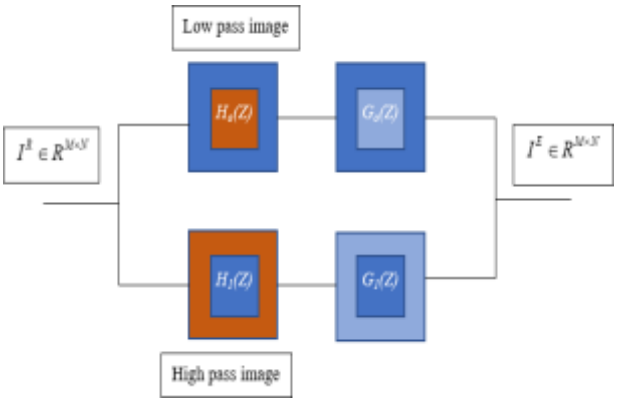

Figure 2. Two-channel decomposition of NSCT pyramid structure

The generated high frequency sub-bands contain the edge details and the noise components. It is important to suppress the noise components and enhance the edge information. The edge details are oftwo types namely, weak edges and strong edges. The objective of image enhancement is to retain the strong edges, highlight the weak edges and remove the noise information. To achieve this, Bayes Shrink threshold is being employed. This threshold is computed as the weighted ratio of noise variance to signal variance. It is represented as,

$$\tau_{BS} = \psi \frac{\sigma^2_{noise}}{\sigma_{signal}} \quad (9)$$

σ^2_{noise} is the variance of noise and σ^2_{signal} is the variance of the signal.

Where $\square$ is a constant factor,

The constant factor was empirically fixed as 0.75 in our work. The noise variance was computed as

$$\frac{Med\left|C_{ij}(l,k)\right|}{0.6} \quad (10)$$

σ_{noise}

Where $C_{ij}^{h}(l,k)$ represents the high frequency coefficient value at the location (i, j) in the level l with the direction k and Med represents the median value. The signal variance is then computed as

σ_{signal}

$$\sqrt{\max(\left|x_{l,k} - \sigma_{noise}^{2}\right|, 0)} \quad (11)$$

Where $x_{l,k}$ is the square of the mean of the high frequency coefficient value in the level l with the direction k .
New enhanced high frequency coefficients are then computed using

$$C^{h}_{ij} = \begin{cases} C^{h}_{ij} & \text{if } C^{h}_{ij} \geq T_{BS} \\ 0 & \text{if } C^{h}_{ij} < T_{BS} \end{cases} \quad (12)$$

Finally, the enhanced *image* $I^{E} \in R^{M \times N}$ is obtained using the low frequency coefficients and the enhanced high frequency coefficients based on inverse NSCT transform.

Segmentation using Hierarchical Fuzzy C Means Gaussian Snake Model (HFC-GSM)Algorithm

A novel algorithm called Hierarchical Fuzzy C Means Gaussian Snake Model (HFC-GSM) algorithm is proposed. In this algorithm modified Snake model based on Gaussian modeling is also employed. In the traditional Snake model, active contours are generated using control points. Here, the initial snake curve is represented as

$$P(s) = [P(s), Q(s), s \in (0,1)] \quad (13$$

This curve is iterated until the following energy function is minimized

$$Egy_{SM} = \int\int \left|I^{2}\right| + \left|h^{2}\left|I(s)\right|\right| ds\,dt \quad (14)$$

Here, Egy_{SM} represents the total energy of traditional Snake model, the first component $\left|I^{2}\right|$ represents the low frequency smoothness energy and the second $\left|h^{2}\left|I(s)\right|\right|$ represents componentthe high frequency edge energy.
In the proposed Gaussian Snake model, a third component based on Gaussian energy is included. Thisnew Gaussian energy function is represented as

$$Egy_{GSM} = \int\int \left|I^{2}\right| + \left|h^{2}\left|I(s)\right|\right| + G_{i,j}\, ds\,dt \quad (15)$$

Where the third component $G_{i,j}$ represents the Gaussian energy component. This is computed as

$$G_{i,j} = e^{\left(\frac{\|i-j\|^{2}}{2sd^{2}}\right)} \quad (16)$$

Where sd represents the standard deviation between the i^{th} and $_j th$ pixel.

The above Gaussian energy function is iterated until convergence state is achieved. The quality of segmentation result obtained mainly depends on the initial values of the energy. To improve the accuracy and reliability of segmentation result, in this work, the initial values are computed using Hierarchical Fuzzy C Means Clustering [28]. That is, the initial values are computed using

$$J = \sum_{i=0}^{255} \sum_{k=1}^{K} \sum_{q=1}^{C} f_{iq} v_{iqk} d(i, q) \quad (17)$$

where f_{iq} refers to the fuzzy membership between pixel x_i and histogram of cluster with center q, v_{iqk} is the sub-membership function that satisfies the condition $\sum_{k=1}^{K} v_{iqk} = 1$ and $d(i, q)$ refers to the sub-distance function between pixel x_i and histogram of cluster with center q. The output of segmentation step is represented as $I^S \in R^{M \times N}$.

Algorithm: Proposed Hierarchical Fuzzy C Means Gaussian Snake Model (HFC-GSM)Algorithm

Input:
Enhanced image $I^E \in R^{M \times N}$.
Output:
Segmented image $I^S \in R^{M \times N}$.
Steps:
Initialize the values of Snake contour using Hierarchical Fuzzy C Means Clustering using Equation (17).
Until Convergence ***do***
Compute the low frequency smoothness energy $\psi \Delta l^2$.
Compute the high frequency edge energy $\Delta h^2 l - \Delta l$.
Gaussian energy component $G_{i,j}$.
Compute the energy of the Gaussian snake model Egy_{GSM} *using Equation (15).*
end

Classification

The above-mentioned segmentation algorithm is used for generation of ROI segments. These segments are extracted from both the benign and malignant images. From these training segments, classification models are created during the training phase. During testing phase the classification is carried out. In this work, a novel Iterative Deep Convolutional Neural Network (IDCNN) is employedfor classification.

Fig.3 shows the architecture of the IDCNN employed in our framework which comprises of four blocks as input block, convolutional block, fully connected block and the classification block. The input features are acquired in the input block. The convolutional block comprises of two convolutional layers. For the first convolutional layer, filters with a size 5×5 were employed. For the next convolutional layer, filters of size 5×5 were used in our framework. The number of filters used was 64 and 128 for the first two layers. The output of this block was given as input to the fully connected block that comprised of one fully connected (FC) layer. The FC block comprised of 4096 nodes. At last, the classification was carried out at the SoftMax layer. The output obtained at this block is considered as final one which may be "1" treated as benign or "2" as malignant. In the proposed IDCNN architecture, training of the input segmented data is done in multiple iterations. At each iteration, small sets of input features are extracted from the segmented images. Thus, the requirement of a larger neural network system is eliminated. The proposed iterative implementation helps in the creation of an adaptive learning model. The features extracted in one iteration are passed on to the next consecutive iteration. This helps in the achievement of higher classification accuracy.

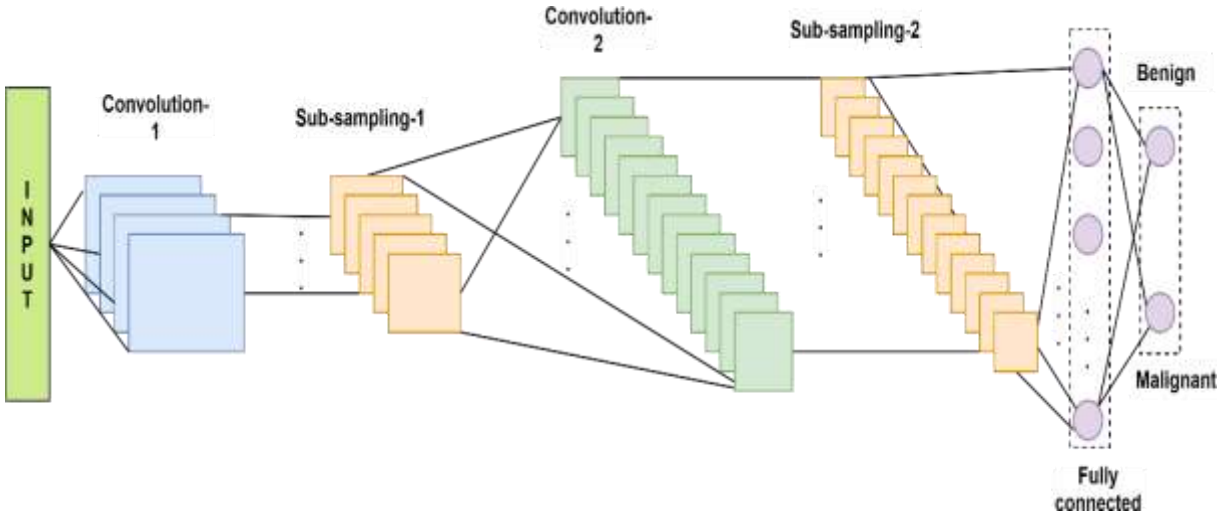

Figure 3. Architecture of the proposed IDCNN structure

4. RESULTS AND DISCUSSION

Simulation parameters

MATLAB [33, 34] is adopted for simulation with windows intel i3 core processor with 6GB RAM configuration. In this work three breast cancer mammogram datasets is utilized for evaluation. These datasets included MIAS dataset [29], CBIS-DDSM dataset [30] and the INbreast dataset [31]. Also opted 10-fold cross validation technique for evaluation the datasets. The initial learning rate for training the proposed IDCNN structure was fixed as 0.01. For every 30 epochs, this rate was reduced to half. This reduction was done until the learning rate got reduced to 10^{-6}.

Simulation Results

Fig.4 shows a sample input noisy breast mammogram image. The image taken is with noise and so it is impossible to process it directly.

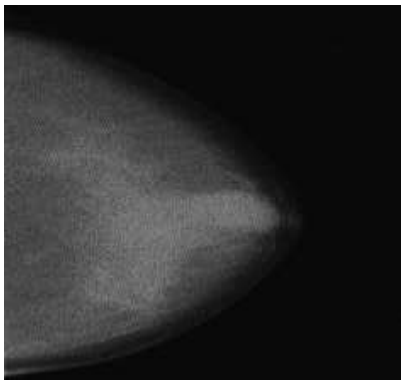

Figure 4. Input noisy mammogram image

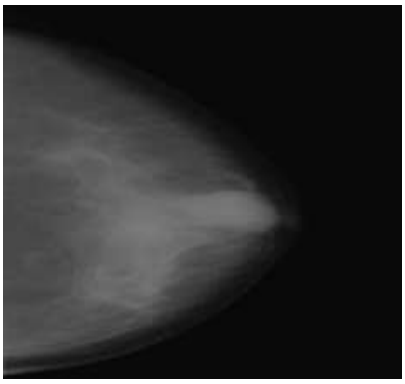

Figure 5. Output of 2D Auto encoder-based Guided Image Filtering

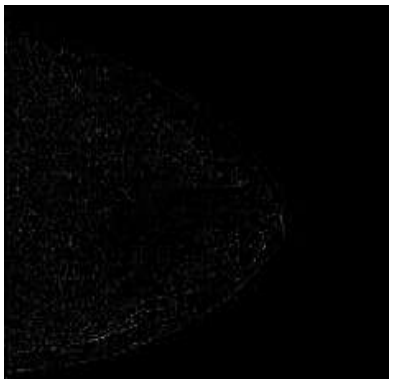

Figure 6. Noisy pixel image

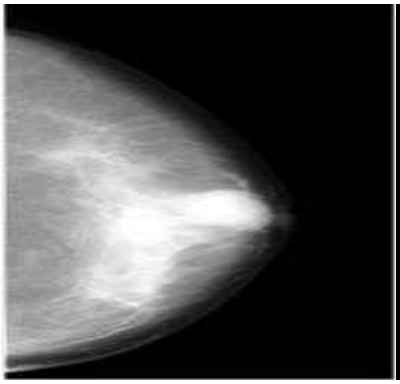

Figure 7 .Output of Bayes Shrink-based Non-Sub-sampled Contourlet Transform

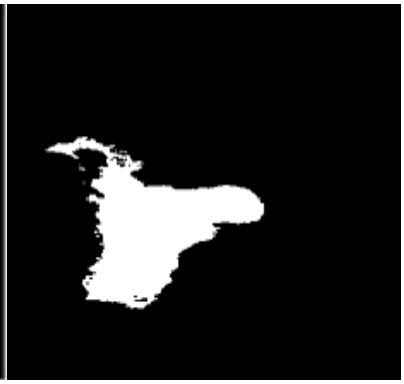

Figure 8. Segmentation resultusing HFC-GSM algorithm

Fig.5 shows the resultant image obtained by the usage of the proposed 2D Auto encoder-based Guided Image Filter (2D AGIF). From fig.6, the filtered image obtained does not have any noisy and hence can be processed easily. Fig.7 shows the corresponding noisy pixel image obtained. Figure 6 shows the enhanced image obtained as a result of enhancement using Bayes Shrink-based Non-Sub- sampled Contourlet Transform (BS-NSCT). This image has enhanced details of the image. Especially, the region of interest is projected in the enhanced image. Fig.8 shows the resultant image obtained after **Hierarchical Fuzzy C Means Gaussian Snake Model (HFC-GSM) Algorithm.** This operation segments the image into different segments. This helps in the identification of region of interest.

Quantitative Analysis

Evaluation of Proposed Restoration Technique

The proposed image restoration using 2D Gaussian Guided Image Filter is evaluated usingmetrics like MSE and PSNR.

Mean Square Error (MSE):

MSE gives the average error value after applying the 2D Gaussian Guided Image filtering algorithm.It is given by

$$(1/N^2)\sum_{i=1}^{N}\sum_{j=1}^{N}[O(i,j)-R(i,j)]^2 \quad (22)$$

Peak Signal-to-Noise Ratio (PSNR):

PSNR gives the ratio of signal value to the error value. Higher the value of PSNR higher will be thesignal quality. It is calculated as

$$PSNR = 10\log_{10}\frac{255^2}{(1/N^2)\sum_{i=1}^{N}\sum_{j=1}^{N}[O(i,j)-R(i,j)]^2} \quad (23)$$

Table 1 shows the performance evaluation using mean square error. From Table 1 see that, the average value of MSE for 2D Median Filter is 8.1. Similarly, the average value of MSE for 2D Adaptive Median Filter is 3.47. However, our proposed 2D Gaussian Guided Image Filter produces a very low MSE of 0.91. Thus, our proposed restoration technique achieves best performance in termsof MSE.

Table 1. Performance evaluation using Mean Square Error

Dataset	MSE		
	MedianFilter	ptive MedianFilter	2D Gaussian GuidedImage Filter
MIAS	8.23	3.08	0.87
CBIS-DDSM	8.17	4.13	0.93
INbreast	7.90	3.20	0.93

Table 2 shows the performance evaluation using peak signal to noise ratio. From Table 2 see that, the average value of PSNR for 2D Median Filter is 20.11. Similarly, the average value of PSNR for 2D Adaptive Median Filter is 23.84. However, our proposed 2D Gaussian Guided Image Filter produces a very high PSNR of 32.76. Thus, our proposed restoration technique achieves best performance in terms of PSNR as well.

Table 2. Performance evaluation using PSNR

Dataset	PSNR (in dB)		
	MedianFilter	ptive MedianFilter	ussian Guided ImageFilter

MIAS	19.02	24.43	32.53
CBIS-DDSM	20.22	23.17	33.14
INbreast	21.11	23.92	32.62

Evaluation of Segmentation Algorithms

Evaluation of the proposed segmentation algorithm Hierarchical Fuzzy C Means Gaussian Snake Model (HFC-GSM) is performed using metrics like Jaccard coefficient, Dice coefficient and Structural Similarity Index.

Jaccard coefficient is commonly used for evaluating the performance of segmentation algorithms. It is given by

$$J(O_a) = \frac{B \cap G}{B \cup G} \quad (24)$$

where O_a is the overlap area, B is the binary image and G is the ground truth image.

Table 3 shows the performance evaluation using Jaccard Coefficient. From Table 3 infer that, the average value of Jaccard Coefficient for K means clustering with Otsu thresholding was 0.4971. Similarly, the average value of Jaccard Coefficient for Fuzzy C Means Clustering with Otsu thresholding was 0.6110. But the proposed Hierarchical Fuzzy C Means Gaussian Snake Model (HFC-GSM) achieved a maximum Jaccard Coefficient of 0.7578. Thus, our proposed framework achieves best performance in terms of Jaccard Coefficient.

Table 3. Performance evaluation using Jaccard Coefficient

Dataset	**Jaccard Coefficient**		
	means clustering + Otsu Thresholding	**Fuzzy C Means Clustering + OtsuThresholding**	**Proposed Hierarchical Fuzzy C Means Gaussian Snake Model (HFC-GSM)**
MIAS	0.5819	0.6219	0.7292
CBIS-DDSM	0.4179	0.5918	0.8048
INbreast	0.4917	0.6193	0.7394

The Dice coefficient is computed as

$$D(B,G) = \frac{2\,|B \cap G|}{|B| + |G|} \quad (25)$$

Its value ranges between 0 to 1. A value of 0 refers to a condition with no overlap and 1 refersto a condition with complete overlap.

Table 4 shows the performance evaluation using Dice Coefficient. From Table 4 infer that, the average value of Dice Coefficient for K means clustering with Otsu thresholding was 0.5588. Similarly, the average value of Dice Coefficient for Fuzzy C Means Clustering with Otsu thresholding was 0.6847. But the proposed Hierarchical Fuzzy C Means Gaussian Snake Model (HFC-GSM) achieved a maximum Dice Coefficient of 0.8067. Hence the proposed methodology provides better results in terms of Dice Coefficient

.

Table 4. Performance evaluation using Dice Coefficient

Dataset	**Dice Coefficient**		
	means clustering +Otsu Thresholding	**Fuzzy C Means Clustering + OtsuThresholding**	**Proposed Hierarchical Fuzzy C Means Gaussian Snake Model (HFC-GSM)**
MIAS	0.5910	0.6292	0.8394
CBIS-DDSM	0.5928	0.7293	0.7304
INbreast	0.4927	0.6957	0.8505

The next metric is Structural Similarity Index (SSIM) [32]. It measures the luminance,contrast and structural similarities between two images and is given by,

$$SSIM = \frac{2\mu_b\mu_g + C_1}{} \quad \frac{2\sigma_{bg} + C_2}{} \tag{26}$$

4832

$$\frac{(2\mu_a\mu_b + C_1)(2\sigma_{ab} + C_2)}{(\mu_a^2 + \mu_b^2 + C_1)(\sigma_a^2 + \sigma_b^2 + C_2)}$$

The default value for C_1 and C_2 are 0.01 and 0.03. The maximum SSIM value is 1.

Table 5 shows the performance evaluation using SSIM Coefficient. From Table 5 infer that, the average value of SSIM Coefficient for K means clustering with Otsu thresholding was 0.6177. Similarly, the average value of SSIM Coefficient for Fuzzy C Means Clustering with Otsu thresholding was 0.7210. But the proposed Hierarchical Fuzzy C Means Gaussian Snake Model (HFC-GSM) achieved a maximum SSIM Coefficient of 0.9125. Thus, our proposed framework achieves best performance in terms of SSIM.

Table 5. Performance evaluation using SSIM Coefficient

Dataset	**SSIM Coefficient**		
	means clustering + Otsu Thresholding	**Fuzzy C Means Clustering + OtsuThresholding**	**Proposed Hierarchical Fuzzy C Means Gaussian Snake Model (HFC-GSM)**
MIAS	0.6293	0.7304	0.9174
CBIS-DDSM	0.6319	0.6934	0.8937
INbreast	0.5921	0.7392	0.9264

Evaluation of Classification Algorithms

To evaluate the classification performance, initially true positive **(** *TP* **)**, true negative **(** *TN* **),** false positive **(** *FP* **)** and false negatives **(** *FN* **)** were computed.

TP **:** It gives the count of malignant cases present and detected.
TN **:** It gives the count of malignant cases not present and not detected.
FP **:** It gives the count of malignant cases not present but detected as malignant.
FN **:** It gives the count of malignant cases present but not detected as malignant.
By using the above calculated parameters value the other classification metrics overall accuracy, recall, precision, specificity and F-Score also calculated.

Table 6. Comparison of Overall Accuracy

Classification algorithms	**Overall accuracy (%)**		
	MIAS	**CBIS-DDSM**	**INbreast**
k-NN	85.34	86.23	85.81
Naïve Bayes	88.23	89.94	87.23
SVM	90.85	91.34	91.94
BPNN	93.21	92.44	94.25
IDCNN	**96.94**	**95.24**	**96.53**

The classification is performed and compared using traditional algorithms. The results for next parameter overall accuracy is tabulated in Table 6. The proposed IDCNN algorithm produces the best results compared to all other traditional classification algorithms.

Fig.9 represents the comparison of specificity for the three datasets. The graph depicts that the average value of specificity obtained by k-NN, Naïve Bayes, SVM, BPNN and IDCNN are 85.35, 89.86, 92.37, 94.33

and 96.25 respectively. Hence it can be concluded as IDCNN outperforms other algorithms.

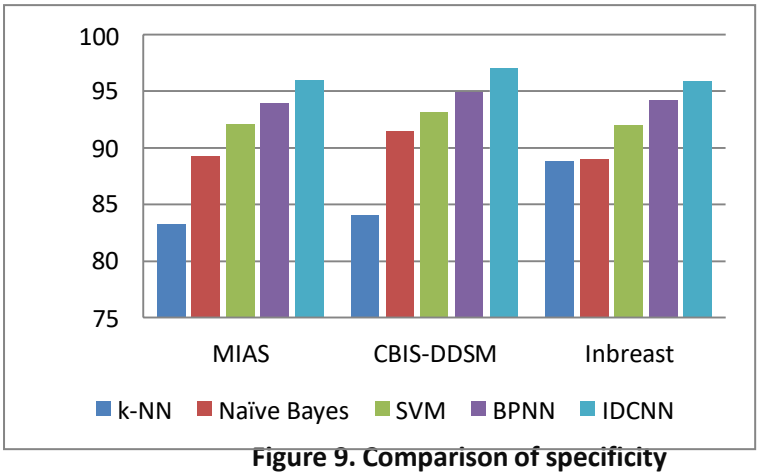

Figure 9. Comparison of specificity

Next Fig.10 represents the comparison of precision for the three datasets and the average value of precision obtained by k-NN, Naïve Bayes, SVM, BPNN and IDCNN are 89.78, 93.22, 93.49, 95.00 and 96.85 respectively. Thus, it is clearly seen that IDCNN outperforms other algorithms.

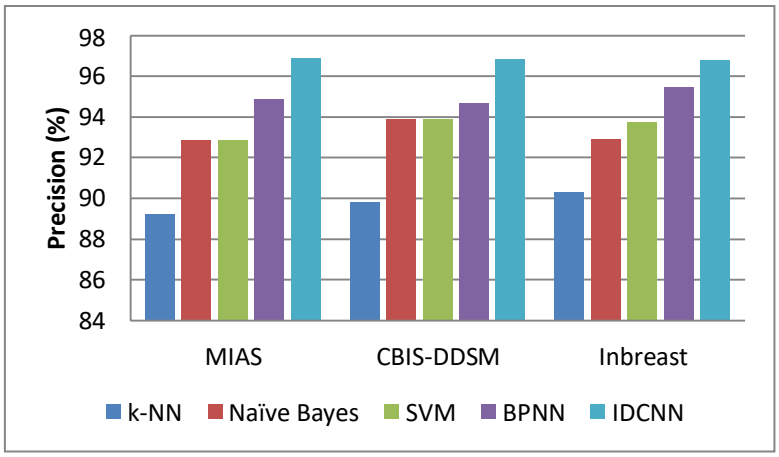

Figure 10. Comparison of precision

Figure 11 shows the comparison of recall for the three datasets. The average value of recall obtained by k-NN, Naïve Bayes, SVM, BPNN and IDCNN are 89.21, 92.04, 93.29, 95.06 and 96.79 respectively. Thus, it is depicts that IDCNN algorithm performance is better than other algorithms.

Recall (%)

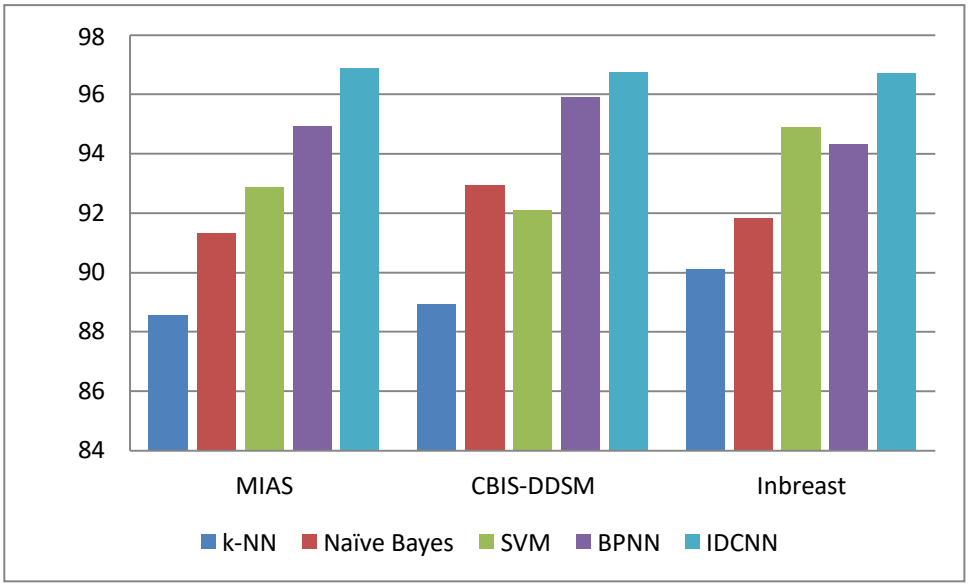

Figure 11. Comparison of recall

Figure 12 represents the comparison of average value of F-score obtained by k-NN, Naïve Bayes, SVM, BPNN and IDCNN which are 91.63, 93.82, 95.15, 95.50 and 97.16 respectively .The results prove that IDCNN performs well than other algorithms.

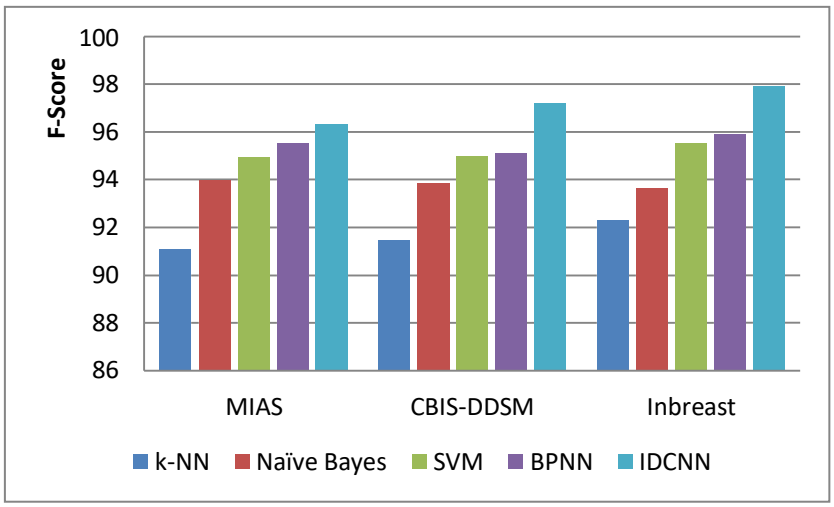

Figure 12. Comparison of F-score

5. CONCLUSION

In this work a novel approach for the segmentation and classification of breast mammogram images are proposed. Noisy images were filtered using a novel 2D Autoencoder-based Guided Image and further enhanced using Bayes Shrink-based NSCT Transform (BS-NSCT). The enhanced images were segmented using a novel Hierarchical Fuzzy C Means Gaussian Snake Model (HFC-GSM) algorithm and Classification was carried out using Deep Convolutional Neural Networks. Quantitative Results are predicted using three datasets. The performance of the proposed filtering algorithm was analyzed using metrics like PSNR and MSE. The proposed filtering algorithm achieved a very low MSE of 0.91 and a very high PSNR of 32.76. The proposed segmentation technique also attained very high values of about 0.7578, 0.8067 and 0.9125 in terms of metrics like Jaccard Coefficient, Dice Coefficient and Structural Similarity index. The DCNN classification algorithm achieved high accuracy of about 96.94, 95.24 and 96.53% for the MIAS, CBIS-DDSM and the INbreast datasets respectively.

References

1. Siegel R.L , Miller K.D, and Jemal.A, “Cancer statistics, 2017,” CA. Cancer J. Clin., vol. 67, no. 1, pp. 7–30, 2017.
2. Gupta, K.K., Vijay, R., Pahadiya, P. et al. Use of Novel Thermography Features of Extraction and Different Artificial Neural Network Algorithms in Breast Cancer Screening. Wireless Pers Commun (2021).
3. Al-antari et al., “An Automatic Computer-Aided Diagnosis System for Breast Cancer in Digital Mammograms via Deep Belief Network,” J. Med. Biol. Eng., vol. 38, no. 3, pp. 443–456, 2018.
4. Al-masni et al., “Simultaneous detection and classification of breast masses in digital mammograms via a deep learning YOLO-based CAD system,” Comput. Methods Programs Biomed., vol. 157, pp. 85–94, 2018.
5. Duraisamy S. and Emperumal S., “Computer-aided mammogram diagnosis system using deep learning convolutional fully complex-valued relaxation neural network classifier,” IET Comput. Vis., vol. 11, no. 8, pp. 656–662, 2017.
6. Al-antari, M. A., Al-masni, M. A., and Kim, T. S. “Deep Learning Computer-Aided Diagnosis for Breast Lesion in Digital Mammogram,” in Advances in Experimental Medicine and Biology, vol. 1213, 2020, pp. 59–72.
7. Wang, Y., Tao, D., Gao, X., Li, X., and Wang, B., “Mammographic mass segmentation: Embedding multiple features in vector-valued level set in ambiguous regions,” in Pattern Recognition, 2011, vol. 44, no. 9, pp. 1903–1915.

*e*ISSN1303-5150

8. Lee, S. K. , et al., "A computer-aided design mammography screening system for detection and classification of microcalcifications," Int. J. Med. Inform., vol. 60, no. 1, pp.29–57, 2000.
9. Al-Masni, M. A. , et al., "Detection and classification of the breast abnormalities in digital mammograms via regional Convolutional Neural Network," in Proceedings of the Annual International Conference of the IEEE Engineering in Medicine and Biology Society, EMBS, 2017, pp. 1230–1233.
10. Vyawahare , A. U. and Thool , V. , "An efficient approach for detection and classification of breast masses in digital mammograms," in 10th International Conference on Advances in Computing, Control, and Telecommunication Technologies, ACT 2019, 2019, pp. 46– 55.
11. Charan, S., Khan, M. J., and Khurshid, K. "Breast cancer detection in mammograms using convolutional neural network," 2018 Int. Conf. Comput. Math. Eng. Technol. Inven. Innov. Integr. Socioecon. Dev. iCoMET 2018 - Proc., vol. 2018–January, pp. 1–5, 2018.
12. Cireşan, D. C., Giusti, A., Gambardella, L. M. and Schmidhuber, J. "Mitosis detection in breast cancer histology images with deep neural networks," in Lecture Notes in Computer Science (including subseries Lecture Notes in Artificial Intelligence and Lecture Notes in Bioinformatics), 2013, vol. 8150 LNCS, no. PART 2, pp. 411–418.
13. Araujo, T. et al., "Classification of breast cancer histology images using convolutional neural networks," PLoS One, vol. 12, no. 6, 2017.
14. Hemavathi, N., Sriranjani, R., Arulmozhi, P. et al. Deep Learning based Early Prediction Scheme for Breast Cancer. Wireless Pers Commun 122, 931–946 (2022). https://doi.org/10.1007/s11277-021-08933-y.
15. Al-antari, M. A., Al-masni, M. A., Choi, M. T., Han, S. M. and Kim, T. S., "A fully integrated computer-aided diagnosis system for digital X-ray mammograms via deep learning detection, segmentation, and classification," Int. J. Med. Inform., vol. 117, no. May, pp. 44–54, 2018.
16. Drukker, K. et al., "Combined Benefit of Quantitative Three-Compartment Breast Image Analysis and Mammography Radiomics in the Classification of Breast Masses in a Clinical Data Set," Radiology, vol. 290, no. 3, pp. 621–628, 2019.
17. Shen, L., Margolies, L. R., Rothstein, J. H., Fluder, E., McBride, R. and Sieh, W. "Deep Learning to Improve Breast Cancer Detection on Screening Mammography," Sci. Rep., vol. 9, no. 1, pp. 1–12, 2019.
18. Manogaran, G., Vijayakumar, V., Varatharajan, R. et al. Machine Learning Based Big Data Processing Framework for Cancer Diagnosis Using Hidden Markov Model and GM Clustering. Wireless Personal Communications 102, 2099–2116 (2018). https://doi.org/10.1007/s11277-017-5044-z.
19. Ting, F. F., Tan, Y. J., and Sim, K. S. "Convolutional neural network improvement for breast cancer classification," Expert Syst. Appl., vol. 120, pp. 103–115, 2019.
20. Akselrod-Ballin, A. et al., "Predicting breast cancer by applying deep learning to linked health records and mammograms," Radiology, vol. 292, no. 2, pp. 331–342, 2019.
21. Geras, K. J., Mann, R. M., and Moy L., "Artificial intelligence for mammography and digital breast tomosynthesis: Current concepts and future perspectives," Radiology, vol. 293, no. 2, pp. 246–259, 2019.
22. Sun, L., Wang, J., Hu, Z, Xu, Y. and Cui, Z., "Multi-View Convolutional Neural Networks for Mammographic Image Classification," IEEE Access, vol. 7, pp. 126273– 126282, 2019.
23. S. Beura, B. Majhi, and R. Dash, "Mammogram classification using two dimensional discrete wavelet transform and gray-level co-occurrence matrix for detection of breast cancer," Neurocomputing, vol. 154, pp. 1–14, 2015.
24. E. Wu, K. Wu, D. Cox, and W. Lotter, "Conditional infilling GANs for data augmentation in mammogram classification," in Lecture Notes in Computer Science (including subseries Lecture Notes in Artificial Intelligence and Lecture Notes in Bioinformatics), 2018, vol. 11040 LNCS, pp. 98–106.

*e*ISSN1303-5150

25. Gautam, A., Bhateja, V., Tiwari, A., and Satapathy, S. C. "An improved mammogram classification approach using back propagation neural network," in Advances in Intelligent Systems and Computing, 2018, vol. 542, pp. 369–376.
26. Hamidinekoo, A., Denton, E., Rampun, A., Honnor, K. and Zwiggelaar, R. "Deep learning in mammography and breast histology, an overview and future trends," Med. Image Anal., vol. 47, pp. 45–67, 2018.
27. Vang, Y. S. , Chen, Z. , and Xie, X., "Deep Learning Framework for Multi-class Breast Cancer Histology Image Classification," in Lecture Notes in Computer Science (includingsubseries Lecture Notes in Artificial Intelligence and Lecture Notes in Bioinformatics), 2018, vol. 10882 LNCS, pp. 914–922.
28. Zheng, Y., Jeon, B., Xu, D., Wu, Q. M. J., and Zhang, H. , "Image segmentation by generalized hierarchical fuzzy C-means algorithm," J. Intell. Fuzzy Syst., vol. 28, no. 2, pp. 961–973, 2015.
29. Suckling et al., "The Mammographic Image Analysis Society Digital Mammogram Database," Expert. Medica, Int. Congr. Ser., vol. 1069, pp. 375–378, 2015.
30. Lee, R. S., Gimenez, F., Hoogi, A., Miyake K. K.,, Gorovoy, M.,and Rubin, D. L., "Data Descriptor: A curated mammography data set for use in computer-aided detection and diagnosis research," Sci. Data, vol. 4, pp. 1–9, 2017.
31. Moreira, I. C., Amaral, I., Domingues, I., Cardoso, A., Cardoso, M. J., and Cardoso, J. S., "INbreast: Toward a Full-field Digital Mammographic Database.," Acad. Radiol., vol. 19,no. 2, pp. 236–248, 2012.
32. Chauhan, N.K., Singh, K. Performance Assessment of Machine Learning Classifiers Using Selective Feature Approaches for Cervical Cancer Detection. Wireless Pers Commun (2022). https://doi.org/10.1007/s11277-022-09467-7.
33. Dhurgadevi, M., Sakthivel, P. An Analysis of Wind Energy Generation by Opting the Better Placement of Wind Turbine by Artificial Neural Network and to Improve the Energy Efficiency of Wireless Sensor Network. Wireless Pers Commun (2021). https://doi.org/10.1007/s11277-021-09255-9.
34. Dhurgadevi, M., Meenakshi Devi, P. An Analysis of Energy Efficiency Improvement Through Wireless Energy Transfer in Wireless Sensor Network. Wireless Pers Commun 98, 3377–3391 (2018). https://doi.org/10.1007/s11277-017-5019-0.

*e*ISSN1303-5150